Original Research

H_2S attenuates oxidative stress via Nrf2/NF-κB signaling to regulate restenosis after percutaneous transluminal angioplasty

Ken Ling[1,2,*], Wei Zhou[3,*], Yi Guo[1], Guofu Hu[1], Jie Chu[1], Fen Xie[1], Yiqing Li[1] and Weici Wang[1]

[1]Department of Vascular Surgery, Union Hospital, Tongji Medical College, Huazhong University of Science and Technology, Wuhan, 430022, China; [2]Department of Anesthesiology, Union Hospital, Tongji Medical College, Huazhong University of Science and Technology, Wuhan, 430022, China; [3]Department of Pancreatic Surgery, Union Hospital, Tongji Medical College, Huazhong University of Science and Technology, Wuhan, 430022, China

Corresponding author: Weici Wang. Email: weiciwang@gmail.com

*These authors contributed equally to this work

Impact statement

This work advances the field of vascular pharmacology as it addresses the issue of neointimal hyperplasia, which is a severe problem that results in restenosis after percutaneous transluminal angioplastic surgery. The effectiveness of vascular surgery is impacted negatively because of this phenomenon, and a solution is urgently needed. Here, we report in a rat model of angioplasty-induced vessel injury that hydrogen sulfide (H_2S) counteracts post-percutaneous transluminal angioplasty neointimal formation and inflammation. Importantly, we demonstrated that the action of H_2S requires Nrf2 signaling and is associated with the regulation of oxidative stress and inflammation via the nuclear factor-kappa B signaling pathway. Notably, our findings offer a potential strategy to address post-vascular surgery restenosis, which remains a clinical problem.

Abstract

Restenosis after angioplasty of peripheral arteries is a clinical problem involving oxidative stress. Hydrogen sulfide (H_2S) participates in oxidative stress regulation and activates nuclear factor erythroid 2-related factor 2 (Nrf2). This study investigated the effect of H_2S and Nrf2 on restenosis-induced arterial injury. Using an *in vivo* rat model of restenosis, we investigated whether H_2S inhibits restenosis after percutaneous transluminal angioplasty (PTA) and the oxidative stress-related mechanisms implicated therein. The involvement of Nrf2 was explored using Nrf2-shRNA. Neointimal formation and the deposition of elastic fibers were assessed histologically. Inflammatory cytokine secretion and the expression of proteins associated with oxidative stress and inflammation were evaluated. The artery of rats subjected to restenosis showed increased arterial intimal thickness, with prominent elastic fiber deposition. Sodium hydrosulfide (NaHS), an H_2S donor, counteracted these changes *in vivo*. Restenosis caused a decrease in anti-oxidative stress signaling. This phenomenon was inhibited by NaHS, but Nrf2-shRNA counteracted the effects of NaHS. In terms of inflammation, inflammatory cytokines were upregulated, whereas NaHS suppressed the induced inflammatory reaction. Similarly, Nrf2 downregulation blocked the effect of NaHS. *In vitro* studies using aortic endothelial and vascular smooth muscle cells isolated from experimental animals showed consistent results as those of *in vivo* studies, and the participation of the nuclear factor-kappa B signaling pathway was demonstrated. Collectively, H_2S played a role in regulating post-PTA restenosis by alleviating oxidative stress, modulating anti-oxidant defense, and targeting Nrf2-related pathways via nuclear factor-kappa B signaling.

Keywords: Hydrogen sulfide, neointimal hyperplasia, nuclear factor erythroid 2-related factor 2, inflammation, anti-oxidant defense

***Experimental Biology and Medicine* 2021; 246: 226–239. DOI: 10.1177/1535370220961038**

Introduction

Revascularization after the occurrence of peripheral vascular disease is usually required for patients with resistance to conservative therapies.[1] To induce revascularization, percutaneous transluminal angioplasty (PTA) is a minimally invasive procedure that is often carried out to treat atherosclerotic lesions in cerebrovascular, peripheral, and coronary vessels.[2] However, the application of PTA is largely limited in peripheral vascular disease because of the high risk of restenosis,[3] which is a major complication of PTA.[4]

Smooth muscle cell proliferation and matrix formation, which result in neointimal hyperplasia, may be key processes in the development of post-PTA restenosis.[5] In addition, negative remodeling, which leads to constriction of an entire vessel, is implicated in post-PTA restenosis.[6]

Oxidative stress is reportedly involved in the development of restenosis. During the treatment of patients with peripheral arterial disease, PTA induces local generation of reactive oxygen species (ROS) such as H_2O_2, which has been shown to stimulate vascular smooth muscle cell growth.[7] Nuclear factor-erythroid 2-related factor 2 (Nrf2) is a leucine zipper redox-susceptible transcription factor that is abundantly expressed in most tissues and regulates the induction of cytoprotective and anti-oxidant genes.[8] Its interaction with the Kelch-like ECH-associated protein 1 system forms a critical cytoprotective mechanism against oxidative stress, with additional functions in reducing inflammation.[9,10] Nrf2 plays essential roles in regulating redox homeostasis and inflammatory conditions, including pulmonary fibrosis, cigarette-induced emphysema, colonic inflammatory injury, and experimental sepsis.[11,12]

As a mediator of Nrf2 signaling, hydrogen sulfide (H_2S) is a potent cardiovascular protective agent responsible for the upregulation of anti-oxidant proteins.[13] Previous studies have shown that increased H_2S bioavailability and Nrf2 activation significantly improved left ventricular function[14] and attenuated tobacco-induced oxidative stress and emphysema in mice.[15] Moreover, deactivation of the nuclear factor-kappa B (NF-κB) signaling pathway has been shown to inhibit restenosis in injured arteries by mediating vascular inflammation.[16] Compounds such as andrographolide[17] and neferine[18] have been shown to suppress arterial restenosis by blocking NF-κB, further accentuating the potential of the NF-κB pathway as a target in anti-restenosis therapy.

We have previously demonstrated the protective effect of H_2S against balloon injury-induced restenosis via Nrf2-related anti-oxidative stress mechanisms.[19] Herein, we speculated that the NF-κB may be involved in the effects of the H_2S/Nrf2 axis in attenuating post-PTA restenosis. To verify this, we constructed an *in vivo* model of restenosis and combined NaHS (a donor of H_2S used to simulate the effects of H_2S) treatment with Nrf2 interference to investigate the regulation of restenosis-induced ROS. *In vitro* studies were correspondingly performed using aortic endothelial cells and vascular smooth muscle cells isolated from experimental animals. In particular, we evaluated the pathological changes induced by post-PTA restenosis and examined the proteins that mediate redox balance and inflammatory response *in vivo* and *in vitro*. The role of NF-κB signaling was elucidated in correlation with the unique functions and mechanisms of H_2S and Nrf2 in attenuating restenosis-induced arterial injury.

Materials and methods

Establishment of in vivo post-PTA restenosis model

All animal experiments were performed in accordance with the National Institute of Health Guide for the Care and Use of Laboratory Animals and were approved by the Animal Experimental Ethical Inspection of the Laboratory Animal Centre, Huazhong Agricultural University (ID: HZAUMO-2017-028). Adult male Sprague Dawley rats ($n = 50$, 250–280 g), which have been routinely used to establish models of restenosis,[20,21] were obtained from Chongqing Medical University (Chongqing, China). The animals were maintained in a specific-pathogen-free laboratory with a regular 12 h/12 h light/dark cycle at an average temperature of 25°C and 40–70% relative humidity. To establish the *in vivo* restenosis model, the animals were randomly divided into five groups ($n = 10$ per group) and subjected to treatment as outlined in Figure 1. Control rats were subjected to sham operation and sacrificed after four weeks (C-4W). For restenosis modeling, rats were subjected to PTA and sacrificed after four weeks (RS-4W). After PTA, the rats were treated with saline (RS-4W + saline), NaHS only (RS-4W + NaHS), or a combination of NaHS and Nrf2-shRNA (RS-4W + Nrf-2-shRNA + NaHS).

To perform PTA, balloon angioplasty of the carotid artery was conducted on the experimental rats, which were anesthetized by intraperitoneal injection of 3% phenobarbital at 40 mg/kg. A balloon catheter was introduced through the right external carotid artery into the aorta, and the balloon was inflated with controlled pressure at 2 atm. The inflated balloon was pushed and pulled through the lumen three times to damage the vessel. After 20 min, the catheter was removed, the artery was ligated, and the wound was closed. Penicillin was applied locally to

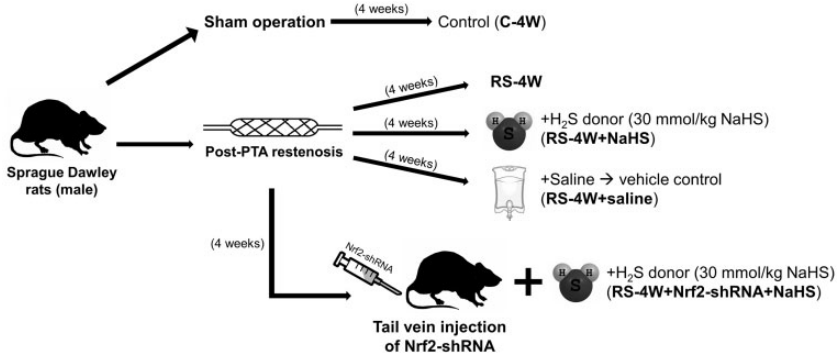

Figure 1. Outline of treatments and groupings for *in vivo* post-PTA restenosis modeling in male Sprague Dawley rats. C-4W: control rats sacrificed at four weeks; RS-4W: post-PTA restenosis modeling for four weeks.

prevent infection. The control rats were anesthetized and underwent surgical procedure without balloon injury. Arterial pressure and heart rate were monitored indirectly using a tail-cuff plethysmographic technique. For experiments involving Nrf2-shRNA, each rat was injected with 4×10^{10} particles of adenoviral Nrf2-shRNA (sequence: GGGTAAGTCGAGAAGTGTTTG) through the tail vein after PTA surgery. NaHS (30 mmol/kg, #13590, Sigma-Aldrich, St. Louis, MO) or saline was administered once a day for four weeks.

Visualization of arterial intima after PTA

After the establishment of the restenosis model, the rats were sacrificed at four weeks for histological and morphometric analyses of the arterial intima. The arterial tissues located in the focus of restenosis (1 cm from the aorta) were removed and quickly fixed in either Bouin's fluid (48 h at room temperature) or 8% formaldehyde in phosphate-buffered saline (PBS, pH 7.4) for 48 h at 4°C. Samples retrieved from the same location were embedded in paraffin blocks at 56°C, and 5-μm-thick serial sections were cut at 1-mm intervals using a Reichert-Jung 2030 microtome. Deparaffinized sections were subjected to hematoxylin and eosin (HE) staining for morphological characterization and Verhoeff's staining for the evaluation of elastic fiber deposition. Image of HE and Verhoeff's staining were captured using an optical microscope at 100× and 200× magnification, respectively. Intimal and medial thicknesses were measured by analyzing three sections from each animal using ImageJ. Ten areas from each cross-sectional HE image were selected while ensuring that the distribution of thicknesses was taken into consideration, and the intimal/medial thickness ratio was calculated.

Determination of the expression of pro-inflammatory cytokines and related factors

Enzyme-linked immunosorbent assay (ELISA) was performed to evaluate the presence of pro-inflammatory factors and related proteins in arterial tissues. The protein levels of interleukin (IL)-1β, IL-6, intercellular cell adhesion molecule (ICAM)-1, and vascular cell adhesion molecule (VCAM)-1 in the plasma were quantified using Quantikine ELISA kits (Elabscience, Wuhan, China) according to the manufacturer's instructions. Absorbance was read at 450 nm using a DR-200Bs microplate reader (Wuxi Hiwell Diatek Instruments Co. Ltd., Wuxi, China).

In vitro cell culture and transfection

For the *in vitro* experiments, rat aortic endothelial cells (RAECs) and rat vascular smooth muscle cells (RVSMCs) were obtained from the thoracic aorta of rats subjected to post-PTA restenosis as previously described.[22,23] The thoracic and abdominal aorta were extracted from the rats under a sterile environment and rinsed three times with PBS. For RAECs, peripheral connective tissue and fat were removed using ophthalmic forceps, and residual blood was rinsed from the arterial lumen. One end of the aorta was sutured with a round needle through a silk thread, which was carefully pulled through the lumen. The arterial intima is flipped and the ends of the artery were ligated with the silk thread. The artery was placed into polylysine-coated T25 flasks with Dulbecco's modified Eagle's medium containing 10% fetal bovine serum, 100 U/mL penicillin, and 100 U/mL streptomycin and cultured for 6 h at 37°C in a humidified environment containing 5% CO_2. After the tissue has adhered, the culture medium was replaced every three days. After two weeks, cells crawling out of the tissue block were collected. For RVSMCs, the middle layer of the thoracic and abdominal aorta was extracted from the rats under a sterile environment and rinsed three times with PBS. The clean tissue block was placed into a Petri dish with 2 mL of high-glucose Dulbecco's modified Eagle's medium containing 10% fetal bovine serum, 100 U/mL penicillin, and 100 U/mL streptomycin and cut into smaller blocks (1 mm × 1 mm × 1 mm) using ophthalmic scissors. The tissues were placed into polylysine-coated T25 flasks and the subsequent steps were the same as those for RAECs. For the *in vitro* experiments, the cells were either treated with various concentrations of H_2S (50, 100, or 200 μmol/L) or transfected with Nrf2 overexpression (Nrf2, sequence GI: 402692377) or interference (Nrf2-siRNA, sequence: GGGTAAGTCGAGAAGTGTTTG) vectors and their respective negative controls (NCs). For Nrf2 overexpression or interference, both cell types were transfected with the Nrf2 overexpression vector (Qiagen, Dusseldorf, Germany) or Nrf2-siRNA (Qiagen), using Lipofectamine 2000 reagent according to the manufacturer's instructions.

Evaluation of RAEC and RVSMC migration and proliferation

RAEC and RVSMC migration was evaluated using a scratch assay. Isolated RAECs or VSMCs were seeded in a six-well plate at 1×10^6 cells/well and cultured overnight. On the next day, a scratch was made swiftly in the cell monolayer in each well using a pipette tip placed perpendicular to the well plate. Unattached cells were washed away with PBS, and the remaining cells in the wells were subjected to the appropriate treatments (H_2S at various concentrations or Nrf2 overexpression/interference) using serum-free medium. Images of the scratched area were acquired immediately (0 h) or 48 h after scratching. The experiment was performed in triplicate and the width of the scratch gap was quantified using ImageJ.

To evaluate cell proliferation, isolated RAECs or RVSMCs were seeded in 96-well plates at 3×10^3 cells/well (100 μL per well) and incubated overnight at 37°C in 5% CO_2 to allow the cells to adhere. The cells were then subjected to the appropriate treatments (H_2S at various concentrations or Nrf2 overexpression/interference) and further cultured for 24, 48, or 96 h. At the indicated time points, 10 μL of 3-(4,5-dimethylthiazol-2-yl)-2,5-diphenyltetrazolium bromide (MTT) reagent (M1025, Solarbio) was added to each well, and the cells were cultured for another 4 h. Thereafter, the liquid was removed from the wells and 150 μL of dimethyl sulfoxide (D2650, Sigma-Aldrich) was added to each well. After 10 min of incubation with

shaking, the absorbance of the wells was measured at 490 nm using a plate reader. The experiment was performed in triplicate.

The 5-ethynyl-2′-deoxyuridine (EdU) cell proliferation assay was performed using the Cell-Light EdU Apollo567 In Vitro Kit (Ribobio) according to the manufacturer's instructions. After the RAECs or RVSCMs were treated in a 96-well plate for the indicated amount of time, 100 μL of 0.05 mmol EdU solution (prepared in culture medium) was added to the cells and incubated for 2 h. Then, 100 μL of fixative solution was added to each well for 30 min, after which 2 mg/mL glycine was added and the plate was gently shaken for 5 min. The fixed cells were washed with PBS and permeabilized with 100 μL of 0.5% Triton X-100 in PBS per well for 10 min. After washing with PBS, 100 μL of 1× Apollo® dye solution was added to each well and the cells were incubated at room temperature in the dark for 30 with gentle shaking. The dye was then removed and the cells were washed three times with 100 μL of 0.5% Triton X-100 in PBS in each well. Nuclear counterstaining was performed by adding 100 μL of Hoechst 33258 solution in each well for 30 min in the dark at room temperature with gentle shaking. The cells were washed three times with PBS and observed under a fluorescence microscope. The percentage of cells showing positive EdU staining was counted and analyzed using ImageJ software.

Evaluation of oxidative stress and inflammation-related signaling

The expression of relevant anti-oxidant factors and inflammation-related NF-κB signaling components was assessed by western blot. Protein extracts (20 μg) prepared from tissue and cell samples were separated by 12% sodium dodecyl sulfate-polyacrylamide gel electrophoresis and transferred to polyvinylidene fluoride membranes (Millipore, MA, USA). The membranes were blocked with 10% milk in Tris-buffered saline (pH 7.6) containing 0.1% Tween-20, incubated with specific antibodies overnight at 4°C, and incubated with horseradish peroxidase-conjugated secondary antibody for 2 h at room temperature. Polyclonal primary antibodies against the following proteins were used: Nrf2 (ab137550, Abcam, Cambridge, UK), heme oxygenase-1 (HO-1, Abcam), glutathione (GSH, Abcam), cystathionine-γ-lyase (CSE, ab80643, Abcam), superoxide dismutase (SOD, Abcam), catalase (CAT, Abcam), NF-κB p65 subunit (ab16502, Abcam), NF-κB p50/105 subunit (ab32360, Abcam), and GAPDH (Cell Signaling Technology, MA, USA). The immunoreactive proteins were visualized using enhanced chemiluminescence (Millipore) and ImageJ software was used for densitometric analysis. The experiment was performed in triplicate.

Statistical analysis

The data were analyzed using OriginPro 8.0 and are expressed as the mean ± standard deviation. Analysis of variance (repeated measures for scratch assay, two-way for MTT and EdU assay, and one-way for all other assays) followed by Tukey's post-hoc multiple comparisons test was performed to compare the means between more than two groups. $P < 0.05$ was considered statistically significant.

Results

H_2S alleviated post-PTA restenosis-induced intimal hyperplasia

Intimal hyperplasia, which is the thickening of the arterial intima, is an indicator of restenosis development. To verify that restenosis was induced and explore the effects of NaHS and Nrf2 on restenosis-induced intimal hyperplasia, histological analysis was performed to evaluate tissue morphology and the distribution of elastic fibers. HE staining (Figure 2(a)) revealed that compared with control rats (C-4W), the arterial intima thickness increased significantly in the artery of rats four weeks post-PTA (RS-4W), confirming the successful induction of restenosis. The administration of NaHS significantly reduced the thickness of the arterial intima, but Nrf2 interference using shRNA did not seem to significantly affect the action of NaHS on neointimal formation, possibly due to insufficient silencing. In terms of elastic fiber deposition, Verhoeff's staining revealed that post-PTA restenosis resulted in a thick layer of dense elastic fibers (Figure 2(b)). While NaHS decreased the thickness of the fiber layer, Nrf2 interference using shRNA counteracted the effect of NaHS. We quantified the intimal (Figure 2(c)) and medial (Figure 2(d)) thickness from the HE images and calculated the intimal/medial ratio (Figure 2(e)) from this data. Post-PTA restenosis caused a remarkable increase in the arterial intimal thickness, whereas NaHS successfully decreased the intimal thickness. There was no difference in terms of medial thickness, but the intimal/medial thickness demonstrated the clear effect of NaHS in reducing neointimal hyperplasia formation post-PTA.

Nrf2 interference blocked the effect of H_2S on redox balance and inflammation in rats subjected to post-PTA restenosis

To determine the effect of Nrf2 and H_2S on oxidative stress, we examined the expression of Nrf2 in the different experimental groups. Nrf2 interference using shRNA caused a significant reduction in the expression of Nrf2, as verified by Figure 3(a) and (b). At four weeks post-PTA, Nrf2 expression was downregulated but was restored by NaHS, whereas Nrf2 interference counteracted the effect of NaHS (Figure 3(c) and (d)). At the same time, we examined the expression of HO-1, GSH, CSE, SOD, and CAT, which are factors involved in anti-oxidant defense. Similar to Nrf2, the expression of the abovementioned proteins was downregulated at four weeks post-PTA, indicating the inhibition of anti-oxidant mechanisms and implying the corresponding promotion of ROS production. However, the expression of these proteins was restored by NaHS, whereas Nrf2 interference greatly suppressed the effect of NaHS.

To determine the effect of Nrf2 and H_2S on inflammatory response, we examined the levels of pro-inflammatory

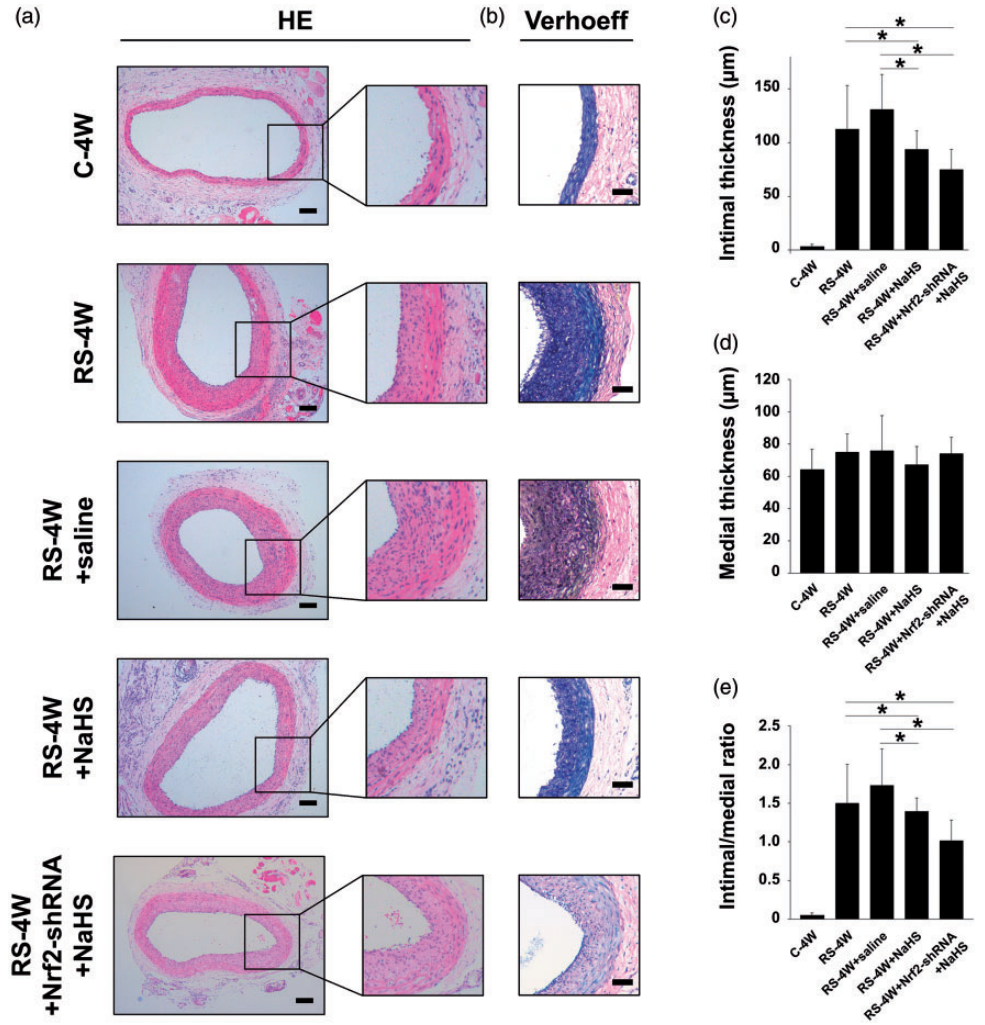

Figure 2. Histological evaluation of rat arteries after percutaneous transluminal angioplasty. (a) HE staining of arterial morphology. The analysis was performed after induction of restenosis, and the arterial intima was stained in rose-pink. Restenosis caused an obvious increase in the intimal thickness, whereas NaHS counteracted this effect. Magnified areas show clear distinction between the intimal and medial layers. Scale bar, 100 μm. (b) Verhoeff's staining of elastic fiber deposition in arterial tissues. The analysis was performed after induction of restenosis, and elastic fibers were stained in blue-black. Scale bar = 50 μm. (c) Intimal and (d) medial thicknesses were measured by selecting 10 areas from each cross-sectional HE image while ensuring that the distribution of thicknesses was taken into consideration, and the (e) intimal/medial thickness ratio was calculated. The data are presented as the mean ± standard deviation ($n = 10$). *$P < 0.05$ (Tukey's post-hoc multiple comparisons test). C-4W: control rats sacrificed at four weeks; RS-4W: post-PTA restenosis modeling for four weeks; HE: hematoxylin and eosin. (A color version of this figure is available in the online journal.)

cytokines IL-1β and IL-6 in the arterial tissues extracted from the different experimental groups (Figure 4). ELISA indicated that the expression of the abovementioned cytokines was upregulated at four weeks post-PTA but was suppressed by NaHS, whereas Nrf2 interference reversed the effect of NaHS. In addition, the expression of VCAM-1 and ICAM-1 was upregulated. NaHS exerted the same effects on VCAM-1 and ICAM-1 as it did on the pro-inflammatory cytokines by suppressing their expression, whereas Nrf2 interference suppressed the effect of NaHS.

H_2S and Nrf2 promoted RAEC migration and proliferation but attenuated those of RVSMCs

Endothelial cell dysfunction contributes to the development of restenosis, wherein the rapid proliferation of vascular smooth muscle cells is a hallmark feature. To investigate the mechanisms of action exerted by Nrf2 and NaHS on post-PTA restenosis *in vitro*, aortic endothelial cells and vascular smooth muscle cells were isolated from rats (RAECs and RVSMCs, respectively) that were subjected to post-PTA restenosis. The RAECs and RVSMCs were then subjected to H_2S treatment (100 μmol/L), Nrf2 overexpression (Nrf2), or Nrf2 interference (Nrf2-siRNA) *in vitro*. Cell response was evaluated using scratch assay for migration and MTT and Edu assay for proliferation. We noticed that RAECs treated with H_2S or Nrf2 migrated more rapidly compared to non-treated control RAECs, closing the scratched gap more efficiently up to 48 h after cell scratching (Figure 5(a) and (b)). However, Nrf2-siRNA did not exert a strong influence on RAEC migration. Concurrently, both H_2S and Nrf2 were able to promote RAEC proliferation for up to 96 h, whereas Nrf2-siRNA suppressed RAEC proliferation (Figure 5(c)

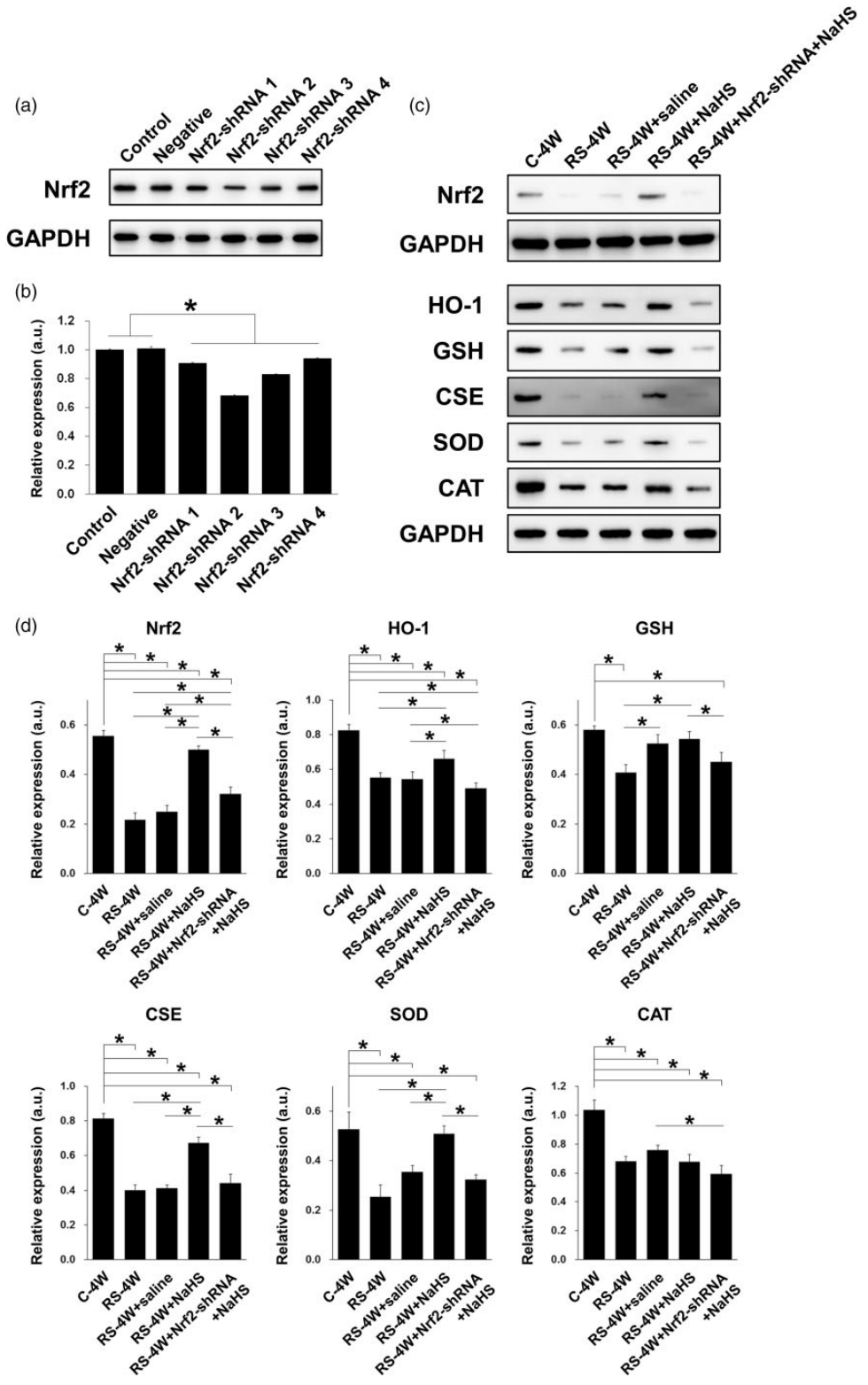

Figure 3. Western blot characterization of Nrf2 and anti-oxidant factors. (a) The expression of Nrf2 in rats after Nrf2-shRNA transfection. Four shRNAs were applied and successful transfection is indicated by the downregulation of Nrf2 expression. (b) Quantification of the results in (a). Nrf2-shRNA 2 was chosen as it showed the highest transfection efficiency. (c) Effect of NaHS and Nrf2 interference on redox balance in rats subjected to post-PTA restenosis. The expression of Nrf2 and the anti-oxidant factors HO-1, GSH, CSE, SOD, and CAT in rats subjected to restenosis and treated with NaHS, with or without Nrf2-shRNA transfection, was measured and quantified. In each case, the level of the anti-oxidant factor was decreased by restenosis, whereas the administration of NaHS significantly upregulated its expression. In addition, the effect of NaHS was attenuated to some degree by the presence of Nrf2-shRNA. (d) Quantification of the protein band gray values. The data are presented as the mean $\pm$ standard deviation ($n = 10$). *$P < 0.05$ (Tukey's post-hoc multiple comparisons test). C-4W: control rats sacrificed at four weeks; RS-4W: post-PTA restenosis modeling for four weeks; HO-1: heme oxygenase-1; GSH: glutathione; CSE: cystathionine-γ-lyase; SOD: superoxide dismutase; CAT: catalase; GAPDH: glyceraldehyde 3-phosphate dehydrogenase.

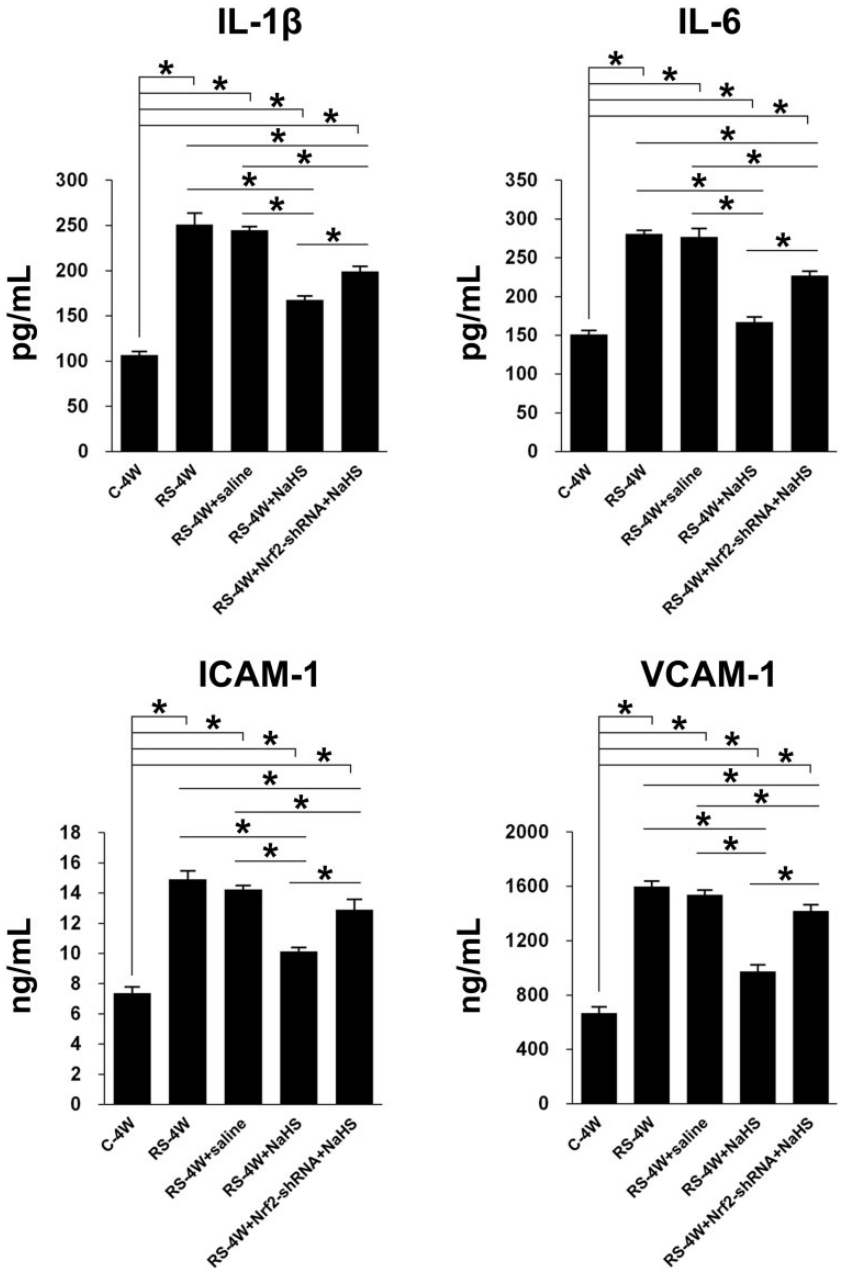

Figure 4. Effect of NaHS and Nrf2 interference on inflammation in rats subjected to post-PTA restenosis. Plasma levels of (a) IL-1β, (b) IL-6, (c) VCAM-1, and (d) ICAM-1 were measured by ELISA and quantified. In each case, the level of the inflammatory factor was increased by restenosis, whereas the administration of NaHS significantly downregulated its expression. In addition, the effect of NaHS was counteracted to some degree by the presence of Nrf2-shRNA. The data are presented as the mean $\pm$ standard deviation ($n = 10$). *$P < 0.05$ (Tukey's post-hoc multiple comparisons test). C-4W: control rats sacrificed at four weeks; RS-4W: post-PTA restenosis modeling for four weeks; IL: interleukin; ICAM-1: intercellular cell adhesion molecule; VCAM-1: vascular cell adhesion molecule.

and (d)). On the other hand, RVSMCs showed the opposite trend as RAECs. Specifically, we observed that H_2S and Nrf2 halted RVSMC migration, resulting in impaired gap closure 48 h after scratching (Figure 5(e) and (f)). Meanwhile, Nrf2-siRNA induced rapid closure of the scratched gap in RVSMCs. In terms of proliferation, H_2S and Nrf2 halted RVSMC proliferation compared to that of control cells, whereas Nrf2-siRNA greatly enhanced RVSMC proliferation for up to 96 h (Figure 5(g) and (h)). Interestingly, these results signify that H_2S administration or Nrf2 overexpression had the ability to restore RAEC function post-PTA while at the same time disrupting the profuse and undesired growth of RVSMCs.

Nrf2 interference disrupted redox and inflammatory signaling in RAECs and RVSMCs

To further understand the role of Nrf2 and NaHS in post-PTA restenosis, *in vitro* investigations were performed to evaluate changes in the redox and inflammatory signaling pathways. Isolated RAECs and RVSMCs were either treated with NaHS (H_2S) at various concentrations

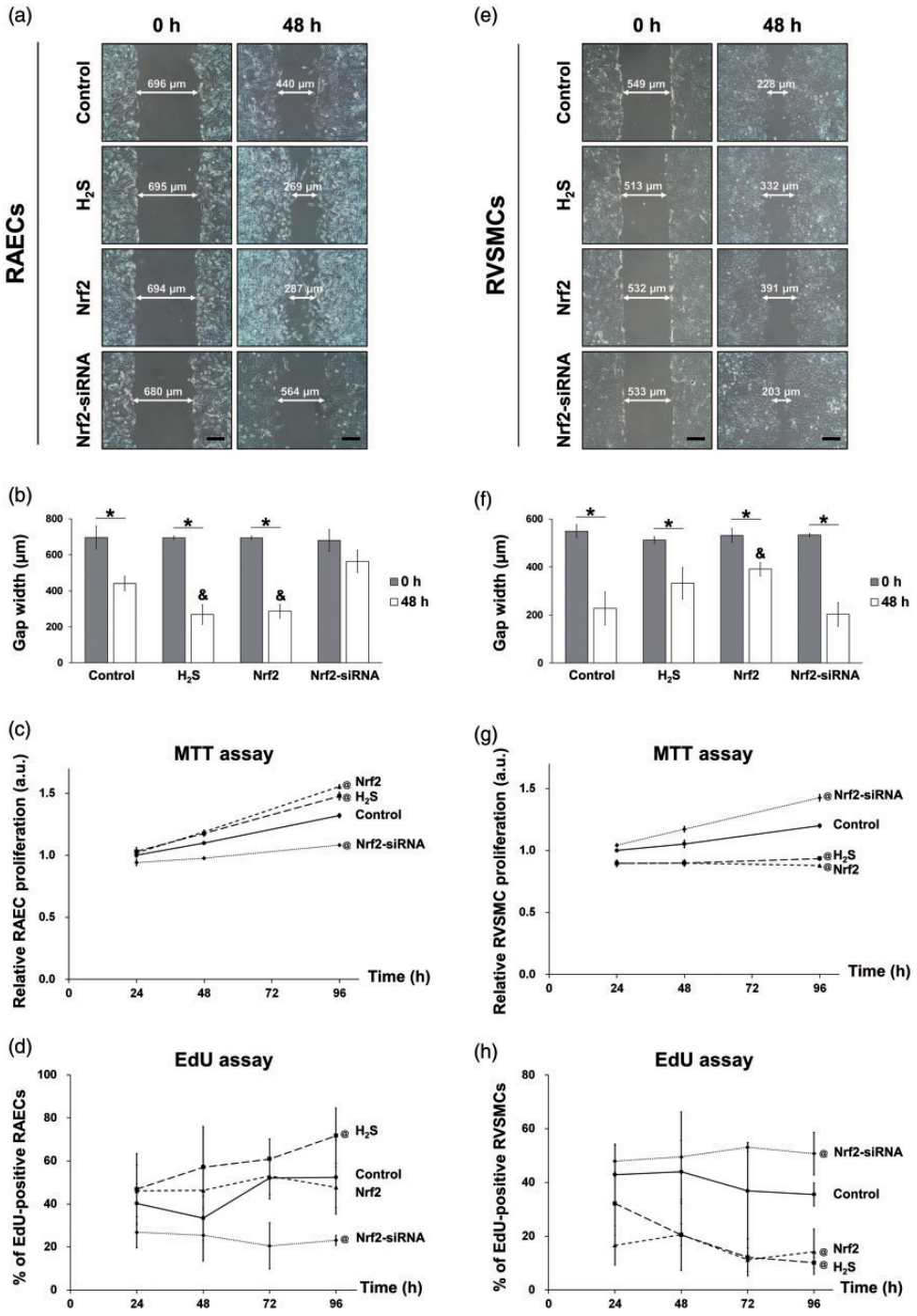

Figure 5. Effect of NaHS and Nrf2 on the migration and proliferation of RAECs and RVSMCs. (a, e) Scratch assay to assess the migration of RAECs and RVSMCs subjected to no treatment (control), H_2S administration (100 μmol/L), Nrf2 overexpression (Nrf2), or Nrf2 interference (Nrf2-siRNA). Images were taken immediately and 48 h after scratching. (b, f) Quantification of gap closure after 48 h of scratching in RAECs and RVSMCs. (c, g) MTT assay of the relative proliferation of RAECs and RVSMCs over 96 h. Absorbance was measured at 24, 48, and 96 h. (d, h) EdU assay of the relative proliferation of RAECs and RVSMCs over 96 h. Absorbance was measured at 24, 48, 72, and 96 h. H_2S and Nrf2 promoted the migration and proliferation of RAECs but inhibited those of RVSMCs, whereas Nrf2-siRNA inhibited the migration and proliferation of RAECs and enhanced those of RVSMCs. The data are presented as the mean ± standard deviation ($n = 3$). $^{*}P < 0.05$ (Tukey's post-hoc multiple comparisons test); $^{\&}P < 0.05$ compared to control at the same time point (Tukey's post-hoc multiple comparisons test); $^{@}P < 0.05$ compared to control at 96 h (Tukey's post-hoc multiple comparisons test). RAECs: rat aortic endothelial cells; RVSMCs: rat vascular smooth muscle cells.

(50, 100, or 200 μmol/L) or transfected with Nrf2 overexpression/interference (Nrf2/Nrf2-siRNA) vectors. Western blot revealed that the expression of Nrf2, HO-1, GSH, CSE, SOD, and CAT was increased by H_2S in a concentration-dependent manner in RAECs (Figure 6(a)) and RVSMCs (Figure 6(b)). In addition, the expression of these factors was upregulated and downregulated by Nrf2 and Nrf2-siRNA, respectively, in both cell types. As an indicator of inflammatory signaling, the p65 and p50/105 subunits of NF-κB, a regulator of inflammatory response, were

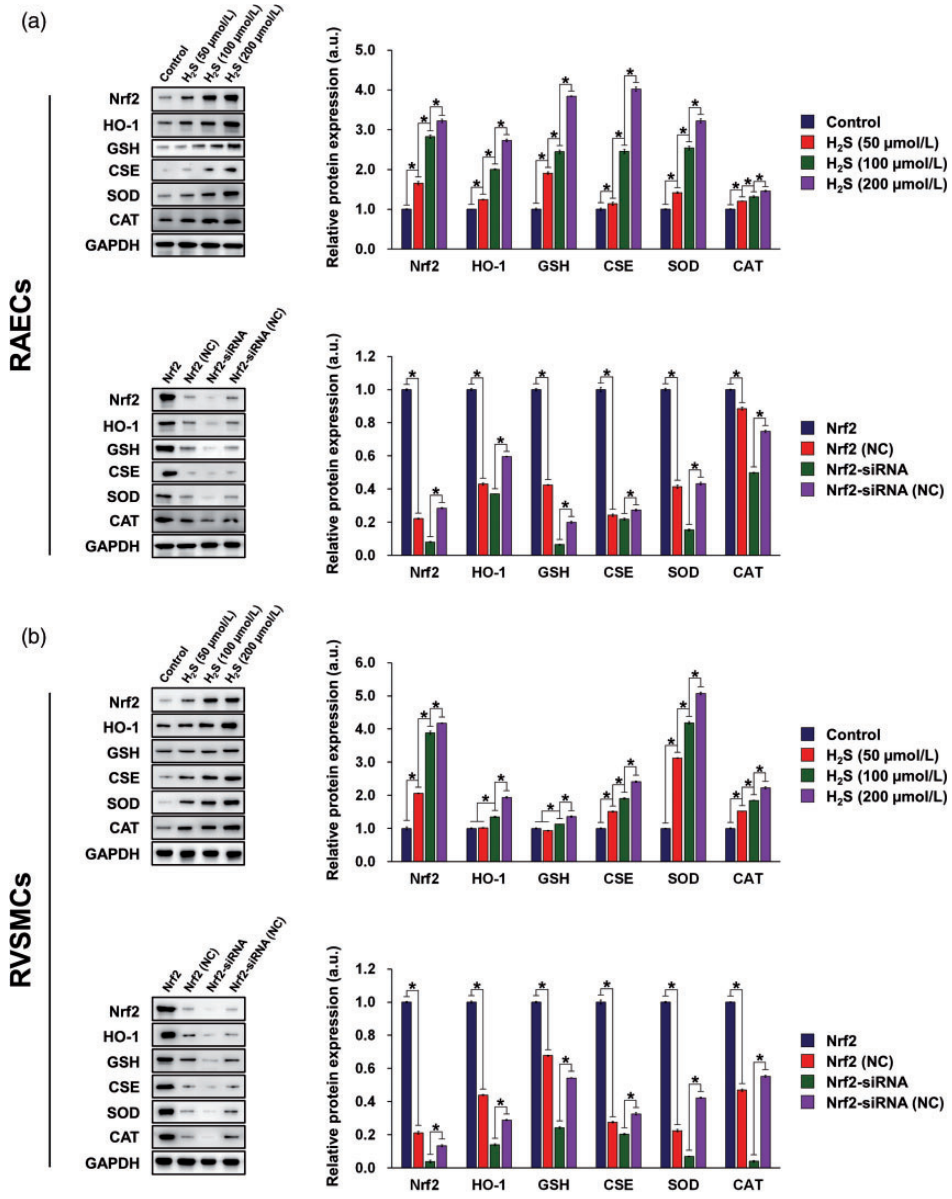

Figure 6. Effect of NaHS and Nrf2 on redox signaling in RAECs and RVSMCs. The expression of Nrf2, HO-1, GSH, CSE, SOD, and CAT after H_2S treatment (50, 100, and 200 μmol/L) or Nrf2 overexpression/interference (with corresponding negative controls, NC) in (a) RAECs and (b) RVSMCs. H_2S reinforced anti-oxidant defense by upregulating the anti-oxidant factors in a concentration-dependent manner. In addition, Nrf2 overexpression (denoted by "Nrf2") evidently upregulated the expression of the measured anti-oxidant factors, whereas Nrf2-siRNA did the opposite compared to the control. The data are presented as the mean ± standard deviation ($n = 3$). *$P < 0.05$ (Tukey's post-hoc multiple comparisons test). RAECs: rat aortic endothelial cells; RVSMCs: rat vascular smooth muscle cells; HO-1: heme oxygenase-1; GSH: glutathione; CSE: cystathionine-γ-lyase; SOD: superoxide dismutase; CAT: catalase; GAPDH: glyceraldehyde 3-phosphate dehydrogenase. (A color version of this figure is available in the online journal.)

subsequently assessed. In accordance with the *in vivo* results of pro-inflammatory cytokine expression, the expression of p65 and p50/105 NF-κB was decreased by H_2S in a concentration-dependent manner in both RAECs (Figure 7(a)) and RVSMCs (Figure 7(b)). In addition, p65 NF-κB was downregulated and upregulated by Nrf2 overexpression and interference, respectively, compared to the NC in both cell types. However, the changes in p50/105 NF-κB induced by Nrf2 overexpression and interference appeared to be inconsistent or random, which may signify that Nrf2 only specifically targeted the p65 subunit of NF-κB and not p50/105.

Discussion

While PTA is widely used in the treatment of cardiovascular diseases because of its high rates of technical success,[24] it exhibits certain limitations. In peripheral, cerebrovascular, and coronary circulation, post-PTA restenosis is a major drawback.[2]Drug-eluting stents have been proposed as a method of addressing the issue of restenosis, but the optimization of stent design to fulfill the requirements of functionality and long-term biological stability remains challenging.[25] Contemporary strategies of combatting restenosis include steroid pulse therapy,[26] viral gene

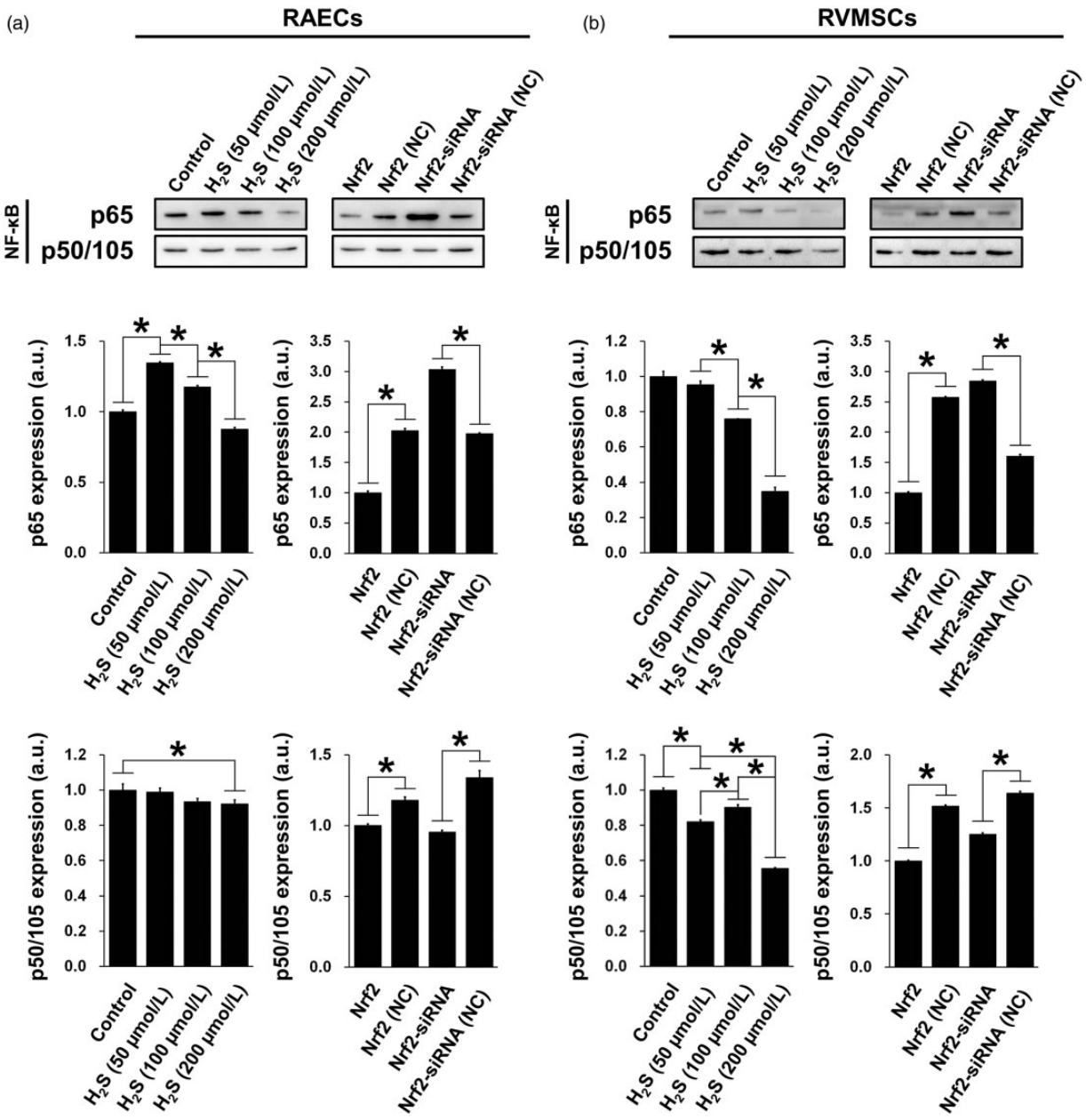

Figure 7. Effect of NaHS and Nrf2 on inflammatory signaling in RAECs and RVSMCs. The expression of NF-κB (subunits p65 and p50/105) after H_2S treatment (50, 100, and 200 μmol/L) or Nrf2 overexpression/interference (with corresponding negative controls, NC) in (a) RAECs and (b) RVSMCs. H_2S alleviated inflammatory response by downregulating p65 and p50/105 NF-κB in a concentration-dependent manner. In addition, Nrf2 overexpression (denoted by "Nrf2") evidently downregulated the expression of p65 NF-κB, whereas Nrf2-siRNA did the opposite compared to the NC. Nrf2 overexpression or interference did not induce consistent trends in the expression of p50/105 NF-κB. The data are presented as the mean $\pm$ standard deviation ($n = 3$). *$P < 0.05$ (Tukey's post-hoc multiple comparisons test). RAECs: rat aortic endothelial cells; RVSMCs: rat vascular smooth muscle cells; NF-κB: nuclear factor-kappa B.

therapy,[27] and targeted nanogel systems of drug delivery.[28] Despite these recent advances, clinical progress remains slow, and effective techniques to prevent the development and exacerbation of restenosis are constantly sought after. We hereby sought a way of mitigating the negative consequences of post-PTA restenosis, such as intimal hyperplasia, ROS production, and inflammation. To this end, we took advantage of chemical agents known to regulate oxidative stress and inflammation, namely Nrf2 and H_2S. ROS generation has been shown to be suppressed by the Nrf2 pathway.[29] In addition, H_2S has been reported as a potent cardiovascular protective agent and plays vital roles in regulating vasodilation, angiogenesis, oxidative stress, and inflammation.[30] We aimed to gain valuable insights on the specific mechanisms through which these agents modulate oxidative stress and the consequential indications on inflammatory response. Thus, our approach involved Nrf2 silencing or interference via shRNA (*in vivo*) and siRNA (*in vitro*) techniques, while NaHS was used as a donor of exogenous H_2S.

We previously demonstrated that NaHS-mediated generation of H_2S exerted protective effects against balloon injury-induced restenosis by preventing neointimal hyperplasia, and this was associated with the activation

of Nrf2/hypoxia-inducible factor 1 signaling.[19] Based on previous work, we herein aimed to further elucidate the regulation of anti-oxidant defense and inflammatory response by Nrf2 in restenosis, specifically focusing on the NF-κB pathway. Through our current study, we observed obvious arterial intimal hyperplasia four weeks after experimental rats were subjected to PTA, which was a sign of restenosis. As anticipated, NaHS effectively reduced the thickness of the arterial intima. We next verified that anti-oxidant defense was weakened in rats subjected to post-PTA restenosis, which was accompanied by elevated inflammatory response. Anti-oxidant defense was successfully restored by NaHS treatment, with concurrent attenuation of inflammatory response. We note also that the effect of NaHS on anti-oxidant defense was partially blocked when Nrf2 was silenced and that NF-κB signaling activation was involved in this process. It is important to point out that the Nrf2 silencing strategy used in our study did not abrogate the protective effect of NaHS against neointimal hyperplasia, contrary to our initial hypothesis. This result was unexpected because although Nrf2 silencing did regulate the markers of oxidative stress, it did not affect neointimal hyperplasia, which is driven by oxidative stress. Thus, we cannot conclude from this work that NaHS protection is directly linked to Nrf2.

A thorough understanding of oxidative stress signaling is crucial as it has been implicated in a variety of pathogenic processes, including those involved in degenerative diseases, atherosclerosis, and inflammation.[31,32] Likewise, the development and progression of restenosis has been shown to involve oxidative stress.[33] Therein, various enzymes and factors participate in ROS scavenging and anti-oxidant defense, including HO-1, GSH, CSE, SOD, and CAT. HO-1 is a redox-sensitive inducible stress protein that degrades heme into CO, iron, and biliverdin[34,35] and possesses the ability to counteract oxidative stress.[36] It is an important component of the intracellular anti-oxidant system,[37] and its activity is usually mediated by inducers related to Nrf2, such as melatonin.[38,39] Similarly, GSH is an anti-oxidant factor that has critical functions in the maintenance of redox homeostasis,[40] whereas CSE is a pyridoxal-5-phosphate-dependent enzyme that produces H_2S through interaction with β-synthase.[41] Furthermore, SOD and CAT are classic anti-oxidant enzymes that protect cells from oxidative damage.[10]

With regards to these anti-oxidant factors, their association with restenosis has been previously reported. Liu *et al.* showed that HO-1 activation alleviated vascular stenosis induced by balloon surgery in rabbits, and the mechanism was related to NF-κB signaling.[42] In a study of post-angioplasty restenosis, Durand *et al.* reported that adenovirus-mediated gene transfer of CAT and SOD was an effective strategy in reducing oxidative stress, inflammation, and restenosis.[43] Vast evidence has also demonstrated the protective effect of these anti-oxidant factors in various types of cells. In particular, resveratrol has been reported to protect human lens epithelial cells against induced H_2O_2-induced oxidative stress by upregulating HO-1, CAT, and SOD-1.[44] Furthermore, it protected lung epithelial cells against cigarette-induced oxidative stress by inducing GSH biosynthesis via the activation of Nrf2.[44] Moreover, fucoidan reduced oxidative stress by upregulating HO-1 and SOD-1,[45] and H_2S is generated predominantly via CSE and is cardioprotective via pathways associated with Nrf2/NF-κB.[46]

Increased expression of anti-oxidant proteins implicates potential resistance to oxidative stress, which may be mediated by Nrf2. In particular, the induction of SOD1, CAT, and HO-1 has been shown to be dependent on the activation of Nrf2 in a study of cardioprotection mediated by proteasome inhibition.[47] Nrf2 activation also reportedly upregulated expression of HO-1, among other anti-oxidant proteins, to impair the growth of smooth muscle cells and attenuate oxidative stress in the aorta of rabbits.[48] We showed *in vivo* and *in vitro* that H_2S treatment resulted in increased Nrf2 expression and enhanced the expression of the aforementioned anti-oxidant factors (HO-1, GSH, CSE, SOD, and CAT) in rats subjected to post-PTA restenosis. This phenomenon is a clear indication of the interplay between H_2S and Nrf2, which may synergistically affect ROS production (Figure 8). In addition, the fact that Nrf2 interference blocked anti-oxidant signaling implicates that in the absence of Nrf2, anti-oxidant factors are unable to exert their full protective effects against ROS-induced cell damage. This consequently supports the hypothesis that Nrf2 is required in anti-oxidant defense and in turn, we can reasonably propose that H_2S is involved in restenosis attenuation through its positive regulatory relationship with Nrf2.

Inflammation has been suggested as a mechanism implicated in restenosis.[49] Thus, anti-inflammatory therapy has been proposed as a way of reducing or preventing

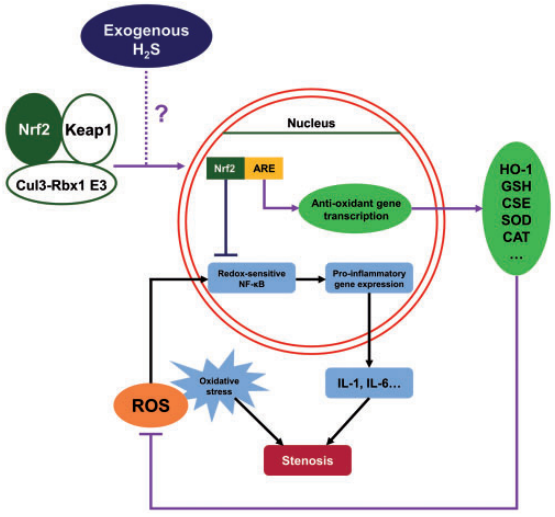

Figure 8. Proposed mechanism through which exogenous H2S mediates Nrf2-induced anti-oxidant defense and attenuates inflammatory signaling. H2S contributes to reduced oxidative stress via nuclear translocation and activation of Nrf2, resulting in the activation of downstream anti-oxidant factors including HO-1, GSH, CSE, SOD, and CAT to lower ROS production. Subsequently, the reduction in ROS levels leads to the inhibition of NF-κB signaling and suppression of pro-inflammatory genes such as interleukins. As a result, restenosis is alleviated. ARE: anti-oxidant response element; ROS: reactive oxygen species; IL: interleukin; HO-1: heme oxygenase-1; GSH: glutathione; CSE: cystathionine-γ-lyase; SOD: superoxide dismutase; CAT: catalase; NF-κB: nuclear factor-kappa B. (A color version of this figure is available in the online journal.)

restenosis.[50] Vascular inflammation was identified as a cornerstone of the restenosis process after balloon angioplasty or stent implantation.[51] In particular, NF-κB participates in the onset of multiple forms of vascular pathobiology, including inflammation.[52,53] These processes are associated with important and well-identified pro-inflammatory cytokines, including IL-1β and IL-6,[54] which consequently increase the protein expression of VCAM-1 and ICAM-1.[55] We further examined the inflammatory response induced by post-PTA restenosis and observed the significant induction of the abovementioned pro-inflammatory cytokines and proteins. The negative regulatory relationship between Nrf2 interference and H_2S in inflammatory signaling is an additional evidence of the positive interplay between Nrf2 and H_2S, which was previously elucidated in the study of oxidative stress signaling. Moreover, the *in vitro* study revealed that H_2S attenuated the expression of NF-κB (p65 and p50/105 subunits) in RAECs and RVSMCs. While Nrf2 overexpression and interference appeared to also regulate p65 NF-κB, the effect of Nrf2 on the p50/105 subunit seemed to be random, suggesting that Nrf2-regulated inflammatory signaling may involve only the p65 but not the p50/105 subunit. Based on previous knowledge of the correlation between NF-κB signaling and inflammatory response, and in conjunction with previous discussions on inflammation, our findings confirm the validity of this proposed correlation. In other words, H_2S and Nrf2 regulate the activity of NF-κB via the p65 subunit, corresponding to diminished inflammatory response.

Our study is limited in several aspects. The major drawback is that the *in vivo* interference strategy did not achieve sufficient silencing of Nrf2 and as a result, the effect of Nrf2-shRNA on neointimal formation and restenosis was not demonstrated. Thus, the hypothesis that NaHS requires Nrf2 to inhibit neointimal hyperplasia was not validated here. Higher doses of viral injection or different interference sequences should be considered in future research to further explore this issue. In addition, healthy rat vessels were injured as a method of creating a model of restenosis, on the basis that neointimal hyperplasia and vessel damage are phenomena involved in real-life cases of restenosis. Establishing the model with atherosclerotic rat vessels or vessels with an existing stenosis would increase the rigor of the model and yield results that are more representative of a clinical restenosis scenario. Furthermore, systemic effects such as blood pressure and systemic oxidative stress were not considered in the current research. As the active agents were administered systemically in the *in vivo* experiments, the sensitivity of the animals to systemic changes may play a part in regulating immune or inflammatory response, in turn affecting the degree of restenosis or neointimal hyperplasia. The three abovementioned issues were not addressed or explored in the current study because of technical limitations that will be included in prospective experimental designs for follow-up studies.

In conclusion, our results demonstrated that H_2S attenuated oxidative stress and inflammation in post-PTA restenosis. We propose that the mechanisms through which H_2S exerts its effects require the participation of the NF-κB signaling pathway. Even though some evidence seems to imply that Nrf2 regulates the anti-oxidant effects of NaHS, the limitations with Nrf2 silencing prevent us from establishing a mechanistic relationship between NaHS, Nrf2, and the development of neointimal hyperplasia. We suggest that H_2S could be a potentially effective agent in preventing the development of post-PTA restenosis, but whether the underlying mechanisms are associated with the upregulation of Nrf2 need to be further investigated and verified.

Authors' contributions: WW conceptualized and designed the study. WZ and GF performed all *in vivo* animal experiments. KL and JC performed all *in vitro* experiments (Western blot, ELISA, scratch assay, MTT assay, and EdU assay). WZ and FX performed all histological staining experiments. WW and YG analyzed the data. KL drafted the manuscript. YL and WW revised and finalized the manuscript. All authors have read and approved the final version of the manuscript.

ACKNOWLEDGMENTS

The data that support the findings of this study are available from the corresponding author upon reasonable request.

DECLARATION OF CONFLICTING INTERESTS

The author(s) declared no potential conflicts of interest with respect to the research, authorship, and/or publication of this article.

FUNDING

The author(s) disclosed receipt of the following financial support for the research, authorship, and/or publication of this article: This work was supported by the National Natural Science Foundation of China (No. 81500376 and 81873529) and Natural Science Foundation of Hubei Province, China (No. 2016CFB108).

ORCID iD

Weici Wang https://orcid.org/0000-0002-1754-5686

REFERENCES

1. Zhou X, Dong J, Zhang L, Liu J, Dong X, Yang Q, Liu F, Liao L. Hyperglycemia has no effect on development of restenosis after percutaneous transluminal angioplasty (PTA) in a diabetic rabbit model. *J Endocrinol* 2015;**224**:119–25
2. Schillinger M, Minar E. Restenosis after percutaneous angioplasty: the role of vascular inflammation. *Vasc Health Risk Manag* 2005;**1**:73–8
3. Hajibandeh S, Hajibandeh S, Antoniou SA, Torella F, Antoniou GA. Treatment strategies for in-stent restenosis in peripheral arterial disease: a systematic review. *Interact Cardiovasc Thorac Surg* 2019;**28**:253–61
4. Fritz P, Stein U, Hasslacher C, Zierhut D, Wannenmacher M, Pritsch M. External beam radiotherapy fails to prevent restenosis after iliac or femoropopliteal percutaneous transluminal angioplasty: results of a prospective randomized double-blind study. *Int J Radiat Oncol Biol Phys* 2004;**59**:815–21
5. Wang X, Li J, Zhang H, Zhang Y. Evaluation of the small intestinal submucosa covered stent in preventing restenosis after percutaneous transluminal angioplasty in the swine. *Eur J Radiol* 2012;**81**:e281
6. Luo H, Nishioka T, Eigler NL, Forrester JS, Fishbein MC, Berglund H, Siegel RJ. Coronary artery restenosis after balloon angioplasty in

humans is associated with circumferential coronary constriction. *Arterioscler Thromb Vasc Biol* 1996;**16**:1393–8
7. Gomez C, Martinez L, Mesa A, Duque JC, Escobar LA, Pham SM, Vazquez-Padron RI. Oxidative stress induces early-onset apoptosis of vascular smooth muscle cells and neointima formation in response to injury. *Biosci Rep* 2015;**35**:e00227
8. Zhao H, Hao S, Xu H, Ma L, Zhang Z, Ni Y, Yu L. Protective role of nuclear factor erythroid 2-related factor 2 in the hemorrhagic shock-induced inflammatory response. *Int J Mol Med* 2016;**37**:1014–22
9. Jin W, Wang H, Yan W, Xu L, Wang X, Zhao X, Yang X, Chen G, Ji Y. Disruption of Nrf2 enhances upregulation of nuclear factor-kappaB activity, proinflammatory cytokines, and intercellular adhesion molecule-1 in the brain after traumatic brain injury. *Mediators Inamm* 2008;**2008**:725174
10. Yang Y, Chen G, Cheng X, Teng Z, Cai X, Yang J, Sun X, Lu W, Wang X, Yao Y, Hu C, Cao P. Therapeutic potential of digitoflavone on diabetic nephropathy: nuclear factor erythroid 2-related factor 2-dependent anti-oxidant and anti-inflammatory effect. *Sci Rep* 2015;**5**:12377
11. Thimmulappa RK, Lee H, Rangasamy T, Reddy SP, Yamamoto M, Kensler TW, Biswal S. Nrf2 is a critical regulator of the innate immune response and survival during experimental sepsis. *J Clin Invest* 2006;**116**:984–95
12. Osburn WO, Karim B, Dolan PM, Liu G, Yamamoto M, Huso DL, Kensler TW. Increased colonic inflammatory injury and formation of aberrant crypt foci in Nrf2-deficient mice upon dextran sulfate treatment. *Int J Cancer* 2007;**121**:1883–91
13. Calvert JW, Jha S, Gundewar S, Elrod JW, Ramachandran A, Pattillo CB, Kevil CG, Lefer DJ. Hydrogen sulfide mediates cardioprotection through Nrf2 signaling. *Circ Res* 2009;**105**:365–74
14. Donnarumma E, Bhushan S, Bradley JM, Otsuka H, Donnelly EL, Lefer DJ, Islam KN. Nitrite therapy ameliorates myocardial dysfunction via H2S and nuclear factor-erythroid 2-related factor 2 (Nrf2)-dependent signaling in chronic heart failure. *J Am Heart Assoc* 2016;**5**:e003551
15. Han W, Dong Z, Dimitropoulou C, Su Y. Hydrogen sulfide ameliorates tobacco smoke-induced oxidative stress and emphysema in mice. *Antioxid Redox Signal* 2011;**15**:2121–34
16. Long G, Lin B, Wang L, Wu L, Yin T, Yu D, Wang G. Sappan lignum extract inhibits restenosis in the injured artery through the deactivation of nuclear factor-κB. *AIMS Bioeng* 2014;**1**:25–39
17. Wang YJ, Wang JT, Fan QX, Geng JG. Andrographolide inhibits NF-kappaBeta activation and attenuates neointimal hyperplasia in arterial restenosis. *Cell Res* 2007;**17**:933–41
18. Jun MY, Karki R, Paudel KR, Sharma BR, Adhikari D, Kim DW. Alkaloid rich fraction from *Nelumbo nucifera* targets VSMC proliferation and migration to suppress restenosis in balloon-injured rat carotid artery. *Atherosclerosis* 2016;**248**:179–89
19. Ling K, Xu A, Chen Y, Chen X, Li Y, Wang W. Protective effect of a hydrogen sulfide donor on balloon injury-induced restenosis via the Nrf2/HIF-1alpha signaling pathway. *Int J Mol Med* 2019;**43**:1299–310
20. Bahnson ES, Kassam HA, Moyer TJ, Jiang W, Morgan CE, Vercammen JM, Jiang Q, Flynn ME, Stupp SI, Kibbe MR. Targeted nitric oxide delivery by supramolecular nanofibers for the prevention of restenosis after arterial injury. *Antioxid Redox Signal* 2016;**24**:401–18
21. Meng Z, Gao P, Chen L, Peng J, Huang J, Wu M, Chen K, Zhou Z. Artificial zinc-finger transcription factor of A20 suppresses restenosis in Sprague Dawley rats after carotid injury via the PPARalpha pathway. *Mol Ther Nucleic Acids* 2017;**8**:123–31
22. Gao DF, Niu XL, Hao GH, Peng N, Wei J, Ning N, Wang NP. Rosiglitazone inhibits angiotensin II-induced CTGF expression in vascular smooth muscle cells – role of PPAR-gamma in vascular fibrosis. *Biochem Pharmacol* 2007;**73**:185–97
23. Wang YY, Chen SM, Li H. Hydrogen peroxide stress stimulates phosphorylation of FoxO1 in rat aortic endothelial cells. *Acta Pharmacol Sin* 2010;**31**:160–64
24. Alfke H, Froelich JJ, Nowak S, Wagner HJ. Cardiovascular risk factors do not predict clinically defined restenosis after percutaneous transluminal angioplasty for lower limb ischemia. *Angiology* 2002;**53**:15–20
25. Rodgers CDK. Drug-eluting stents: role of stent design, delivery vehicle, and drug selection. *Rev Cardiovasc Med* 2002;**3**:S10–15
26. Yokota K, Uchida H, Tanano A, Shirota C, Tainaka T, Hinoki A, Murase N, Oshima K, Shirotsuki R, Chiba K. Steroid pulse therapy prevents restenosis following balloon dilatation for esophageal stricture. *Pediatr Surg Int* 2016;**32**:875–9
27. Hall S, Agrawal DK. Delivery of viral vectors for gene therapy in intimal hyperplasia and restenosis in atherosclerotic swine. *Drug Deliv Transl Res* 2018;**8**:918–27
28. Yang Q, Peng J, Chen C, Xiao Y, Tan L, Xie X, Xu X, Qian Z. Targeting delivery of rapamycin with anti-collagen IV peptide conjugated Fe(3)O(4)@nanogels system for vascular restenosis therapy. *J Biomed Nanotechnol* 2018;**14**:1208–24
29. Kim SJ, Park C, Han AL, Youn MJ, Lee JH, Kim Y, Kim ES, Kim HJ, Kim JK, Lee HK, Chung SY, So H, Park R. Ebselen attenuates cisplatin-induced ROS generation through Nrf2 activation in auditory cells. *Hear Res* 2009;**251**:70–82
30. Yu XH, Cui LB, Wu K, Zheng XL, Cayabyab FS, Chen ZW, Tang CK. Hydrogen sulfide as a potent cardiovascular protective agent. *Clin Chim Acta* 2014;**437**:78–87
31. Valko M, Leibfritz D, Moncol J, Cronin MT, Mazur M, Telser J. Free radicals and antioxidants in normal physiological functions and human disease. *Int J Biochem Cell Biol* 2007;**39**:44–84
32. Codoner-Franch P, Valls-Belles V, Arilla-Codoner A, Alonso-Iglesias E. Oxidant mechanisms in childhood obesity: the link between inflammation and oxidative stress. *Transl Res* 2011;**158**:369–84
33. Kochiadakis GE, Arfanakis DA, Marketou ME, Skalidis EI, Igoumenidis NE, Nikitovic D, Giaouzaki A, Chlouverakis G, Vardas PE. Oxidative stress changes after stent implantation: a randomized comparative study of sirolimus-eluting and bare metal stents. *Int J Cardiol* 2010;**142**:33–7
34. Zhang J, Fu B, Zhang X, Zhang L, Bai X, Zhao X, Chen L, Cui L, Zhu C, Wang L, Zhao Y, Zhao T, Wang X. Bicyclol upregulates transcription factor Nrf2, HO-1 expression and protects rat brains against focal ischemia. *Brain Res Bull* 2014;**100**:38–43
35. Ling K, Men F, Wang WC, Zhou YQ, Zhang HW, Ye DW. Carbon monoxide and its controlled release: therapeutic application, detection, and development of carbon monoxide releasing molecules (CORMs). *J Med Chem* 2018;**61**:2611–35
36. Kim DS, Chae SW, Kim HR, Chae HJ. CO and bilirubin inhibit doxorubicin-induced cardiac cell death. *Immunopharmacol Immunotoxicol* 2009;**31**:64–70
37. Hwang YP, Jeong HG. The coffee diterpene kahweol induces heme oxygenase-1 via the PI3K and p38/Nrf2 pathway to protect human dopaminergic neurons from 6-hydroxydopamine-derived oxidative stress. *FEBS Lett* 2008;**582**:2655–62
38. Kim KM, Pae HO, Zheng M, Park R, Kim YM, Chung HT. Carbon monoxide induces heme oxygenase-1 via activation of protein kinase R-like endoplasmic reticulum kinase and inhibits endothelial cell apoptosis triggered by endoplasmic reticulum stress. *Circ Res* 2007;**101**:919–27
39. Negi G, Kumar A, Sharma SS. Melatonin modulates neuroinflammation and oxidative stress in experimental diabetic neuropathy: effects on NF-kappaB and Nrf2 cascades. *J Pineal Res* 2011;**50**:124–31
40. Aoyama K, Nakaki T. Glutathione in cellular redox homeostasis: association with the excitatory amino acid carrier 1 (EAAC1). *Molecules* 2015;**20**:8742–58
41. Huang CY, Yao WF, Wu WG, Lu YL, Wan H, Wang W. Endogenous CSE/H2 S system mediates TNF-alpha-induced insulin resistance in 3T3-L1 adipocytes. *Cell Biochem Funct* 2013;**31**:468–75
42. Liu D, Mo X, Zhang H, Wu L, Tan J, Xiao J, Qin Z. Heme oxygenase-1 (HO-1) alleviates vascular restenosis after balloon injury in a rabbit carotid artery model. *Int J Clin Exp Pathol* 2018;**11**:2479–87
43. Durand E, Al Haj Zen A, Addad F, Brasselet C, Caligiuri G, Vinchon F, Lemarchand P, Desnos M, Bruneval P, Lafont A. Adenovirus-mediated gene transfer of superoxide dismutase and catalase decreases restenosis after balloon angioplasty. *J Vasc Res* 2005;**42**:255–65
44. Zheng Y, Liu Y, Ge J, Wang X, Liu L, Bu Z, Liu P. Resveratrol protects human lens epithelial cells against H_2O_2-induced oxidative stress by increasing catalase, SOD-1, and HO-1 expression. *Mol Vis* 2010;**16**:1467–74

45. Ryu MJ, Chung HS. Fucoidan reduces oxidative stress by regulating the gene expression of HO1 and SOD1 through the Nrf2/ERK signaling pathway in HaCaT cells. *Mol Med Rep* 2016;**14**:3255–60
46. Zheng J, Zhao T, Yuan Y, Hu N, Tang X. Hydrogen sulfide (H2S) attenuates uranium-induced acute nephrotoxicity through oxidative stress and inflammatory response via Nrf2-NF-kappaB pathways. *Chem Biol Interact* 2015;**242**:353–62
47. Dreger H, Westphal K, Weller A, Baumann G, Stangl V, Meiners S, Stangl K. Nrf2-dependent upregulation of antioxidative enzymes: a novel pathway for proteasome inhibitor-mediated cardioprotection. *Cardiovasc Res* 2009;**83**:354–61
48. Levonen AL, Inkala M, Heikura T, Jauhiainen S, Jyrkkanen HK, Kansanen E, Maatta K, Romppanen E, Turunen P, Rutanen J, Yla-Herttuala S. Nrf2 gene transfer induces antioxidant enzymes and suppresses smooth muscle cell growth in vitro and reduces oxidative stress in rabbit aorta in vivo. *Arterioscler Thromb Vasc Biol* 2007;**27**:741–7
49. Drachman DE, Simon DI. Inflammation as a mechanism and therapeutic target for in-stent restenosis. *Curr Atheroscler Rep* 2005;**7**:44–9
50. Donners MM, Daemen MJ, Cleutjens KB, Heeneman S. Inflammation and restenosis: implications for therapy. *Ann Med* 2003;**35**:523–31
51. Okamoto E, Couse T, De Leon H, Vinten-Johansen J, Goodman RB, Scott NA, Wilcox JN. Perivascular inflammation after balloon angioplasty of porcine coronary arteries. *Circulation* 2001;**104**:2228–35
52. Liu T, Zhang L, Joo D, Sun SC. NF-kappaB signaling in inflammation. *Signal Transduct Target Ther* 2017;**2**:17023
53. Tak PP, Firestein GS. NF-kappaB: a key role in inflammatory diseases. *J Clin Invest* 2001;**107**:7–11
54. Aly H, Khashaba MT, El-Ayouty M, El-Sayed O, Hasanein BM. IL-1beta, IL-6 and TNF-alpha and outcomes of neonatal hypoxic ischemic encephalopathy. *Brain Dev* 2006;**28**:178–82
55. Kim I, Moon SO, Kim SH, Kim HJ, Koh YS, Koh GY. Vascular endothelial growth factor expression of intercellular adhesion molecule 1 (ICAM-1), vascular cell adhesion molecule 1 (VCAM-1), and E-selectin through nuclear factor-kappa B activation in endothelial cells. *J Biol Chem* 2001;**276**:7614–20

(Received April 25, 2020, Accepted September 2, 2020)